A micromechanical model for predicting the fracture toughness of functionally graded foams

Seon-Jae Lee [1], Junqiang Wang [1], Bhavani V. Sankar *

Department of Mechanical and Aerospace Engineering, P.O. Box 116250, University of Florida, Gainesville, FL 32611-6250, USA

Abstract

In this paper, finite element method based micromechanical analysis is used to understand the fracture behavior of functionally graded foams. The finite element analysis uses a micro-mechanical model in conjunction with a macro-mechanical model in order to relate the stress intensity factor to the stresses in the struts of the foam. The stress intensity factor at the crack tip of the macro-mechanical model can be evaluated using either the *J*-contour integral or the stresses in the singularity-dominated zone. The fracture toughness is evaluated for various crack positions and length within the functionally graded foam. Then the relationship between the fracture toughness of the graded foam and the local density at the crack tip is studied. Convergence tests for both macro-mechanical and micro-mechanical model analysis were conducted in order to maintain adequate accuracy with reasonable computational time. Fracture toughness of homogenous foams and functionally graded foams for various cases are presented as a function of relative density. This study indicates that the fracture toughness of functionally graded foams mainly depends on the relative density at the crack-tip.
© 2006 Elsevier Ltd. All rights reserved.

Keywords: Cellular materials; Fracture simulation; Fracture toughness; Functionally graded materials; Graded foams; Inhomogeneous foams; Micromechanics

1. Introduction

The microstructure of cellular solids such as metallic and carbon foams can be tailored to obtain optimum performance for use in multi-functional structures. Such multi-functional structures can be used in integral load-carrying thermal protection systems for hypersonic vehicles due to their low thermal conductivity, increased strength and stiffness. An excellent treatise on structure and properties of cellular solids can be found in Gibson and Ashby (1998). They have presented approximate formulas for Mode I fracture toughness of cellular solids as a function of relative density and the strength of the strut or cell wall material. Choi and Sankar (2003, 2005) found that the Mode I and II fracture toughness of cellular solids strongly depend on the

---

* Corresponding author. Tel.: +1 352 392 6749; fax: +1 352 392 7303.
  E-mail address: sankar@ufl.edu (B.V. Sankar).
[1] Graduate student.

relative-density; however the cell spacing and strut dimensions also have an effect on the fracture toughness. Although significant work has been done in modeling homogeneous cellular materials, models for functionally graded foams or graded cellular materials, especially for strength and fracture toughness, are at their infancy, and it will be the main focus of this paper. Functionally graded foams can be made by controlling the size of the voids in the porous medium. The density can be varied either by changing the unit-cell dimensions or strut cross-section or both. Graded foams can also be manufactured by dispersing hollow micro-balloons of varying sizes in a matrix medium (Madhusudhana et al., 2004). In this paper, both cases—varying wall thickness and varying unit-cell dimensions—are considered independently using a finite element based micro-mechanical analysis. The finite element analysis uses a micro-mechanical model in conjunction with a macro-mechanical, or simply macro-model, in order to relate the stress intensity factor to the stresses in the struts of the foam. The stress intensity factor of the macro-model at the crack tip is evaluated using the J-contour integral. The fracture toughness is evaluated for various crack positions and crack lengths within the functionally graded foam. Then the relationship between the fracture toughness of the functionally graded foam and the local density at the crack tip is studied. In addition, convergence tests for both macro- and micro-models were conducted. The results will help in understanding the fracture behavior of functionally graded foams.

2. Overview of the procedures

The method of determining the fracture toughness of the graded foam described in this paper is similar to that discussed by Choi and Sankar (2003, 2005) for homogeneous foams. In the present case, the cellular material is inhomogeneous in the macro-scale. That is, the microstructure is graded and the foam is treated as a functionally graded material in macro-scale. The foam can be modeled either as an inhomogeneous continuum, or as a frame consisting of beam elements to model the struts. The former model (continuum model) will be referred to as the macro-model and the latter (frame model) as the micro-model. In the finite element analysis solid element are used in the macro-model and beam elements in the micro-model.

We create the crack in the foam by removing a set of struts along the intended crack surface. We consider a portion of the foam surrounding the crack tip for the micro-model (see Fig. 1). The dimensions of the micro-model should be much larger than the cell size (strut spacing) so that it can be considered as a continuum. Then we apply displacements to the boundary nodes of the micro-model such that a known stress intensity factor (SIF) exists at the crack tip. The maximum stresses in the struts in the vicinity of the crack tip are calculated from the FE micro-model. From the failure criterion for the strut material, one can calculate the maximum stress intensity factor that will cause the failure of the crack tip struts, and thus causing crack propagation in a macro-scale sense. The key thing in this approach is to be able to calculate the SIF for a given
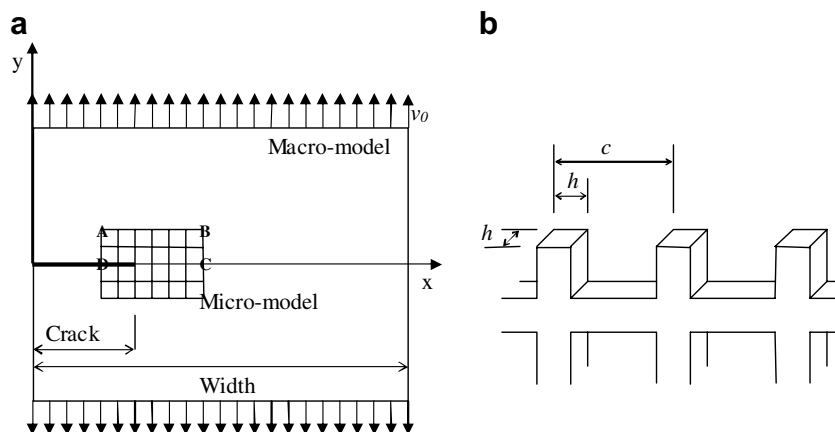

Fig. 1. (a) Macro-model consists of plane 8-node solid elements. The region in the middle with grids indicates the portion used in the micro-model. (b) The micro-model consists of frame elements to model the individual struts. The displacements from the macro-model are applied as boundary conditions in the micro-model.

boundary displacements or apply a set of boundary conditions that corresponds to a given stress intensity factor in the macro-scale sense.

For this purpose we turn to the macro-model as shown in Fig. 1. In the macro-model a much larger size of the foam is modeled using continuum elements, in the present case, plane solid elements. The micro-model is basically embedded into the macro-model. The foam is subjected to an arbitrary boundary condition to produce a given mode-mixity at the crack tip. In this paper, we consider only Mode I symmetric loading (mode-mixity = 0). The stress intensity factor at the crack tip is calculated either from the crack-tip stress field or the J-integral. The displacements of points along the boundary of the micro-model are obtained from the FE analysis of the macro-model and applied to the boundary of the micro-model as explained in the preceding paragraph.

It should be noted that the aforementioned macro-model was not necessary in the case of homogeneous foams (Choi and Sankar, 2003). Closed-form expressions for crack-tip displacement field are available for orthotropic materials (Sih and Liebowbitz, 1968), and hence the displacement boundary conditions for the micro-model for a given SIF are easily obtained.

3. Estimation of continuum properties

The macro-model of the graded foam requires continuum properties at each point or at least for each element in the finite element model. In the following, we briefly describe the procedures to calculate the continuum properties of a homogeneous cellular medium and then extend the idea to graded foams.

3.1. Homogeneous foam

Most of the open-cell foams can be considered as orthotropic materials. Choi and Sankar (2005) derived the elastic constants of homogeneous foams in terms of the strut material properties and unit-cell dimensions. In their model they assumed that the strut has a square cross-section and the unit-cell is a cube. In the present approach we would like to consider a general case wherein the unit-cell is a rectangular parallelepiped of dimensions $c_1 \times c_2 \times c_3$. The derivation of formulas for the density and Young's modulus are straightforward and they are as follows:

$$\frac{\rho^*}{\rho_s} = \frac{(c_1 + c_2 + c_3)h^2 - 2h^3}{c_1 c_2 c_3} \tag{1}$$

$$E_1^* = \left(\frac{h^2}{c_2 c_3}\right)E_s, \quad E_2^* = \left(\frac{h^2}{c_1 c_3}\right)E_s, \quad E_3^* = \left(\frac{h^2}{c_1 c_2}\right)E_s \tag{2}$$

where a superscript * denotes the foam properties and a subscript s denotes the solid properties or the strut properties.

The derivation of shear modulus is slightly involved and it is described below. We show the derivation of the shear modulus G_{12}^* from the unit-cell dimensions, strut cross-sectional dimensions and the strut Young's
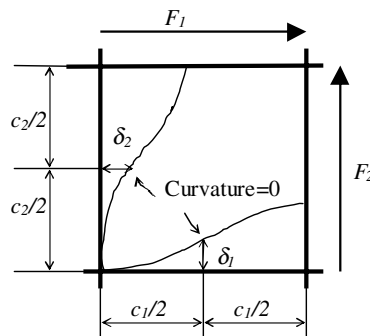

Fig. 2. Flexural deformation of struts under shear stresses.

modulus. When a shear stress is applied, struts are deformed as shown in Fig. 2. Bending moment becomes zero at the middle of struts because the curvatures are zero due to symmetry. The struts are assumed as a beam fixed at the end with a concentrated force at the middle at a distance $\frac{c_1}{2}$ and $\frac{c_2}{2}$, respectively from the fixed end as shown in Fig. 2. The maximum displacement can be written as,

$$\delta_1 = \frac{PL^3}{3EI} = \frac{F_2\left(\frac{c_1}{2}\right)^3}{3E_sI} \text{ and } \delta_2 = \frac{PL^3}{3EI} = \frac{F_1\left(\frac{c_2}{2}\right)^3}{3E_sI} \tag{3}$$

$$\text{where } I = \frac{bh^3}{12} = \frac{h^4}{12}$$

The applied shear stress can be written as $\tau_{12}^* = \frac{F_1}{c_1c_3} = \frac{F_2}{c_2c_3}$. Using the relations, $\frac{F_1}{c_1} = \frac{F_2}{c_2}$, the maximum displacements (Eq. (3)) can be rewritten as

$$\delta_1 = \frac{c_1^3 F_2}{24E_sI} \text{ and } \delta_2 = \frac{c_1c_2^2 F_2}{24E_sI} \tag{4}$$

The shear strain γ_{12} can be derived as

$$\gamma_{12} = \frac{2\delta_2}{c_2} + \frac{2\delta_1}{c_1} = \frac{2c_1\delta_2 + 2c_2\delta_1}{c_1c_2} \tag{5}$$

Using Eq. (4), the shear strain can be written as,

$$\gamma_{12} = \frac{(c_1c_3 + c_1^2)F_3}{12E_sI} \tag{6}$$

The shear modulus G_{12}^* can be derived as

$$G_{12}^* = \frac{\tau_{12}^*}{\gamma_{12}} = \frac{\frac{F_2}{c_2c_3}}{\frac{(c_1c_2+c_1^2)F_3}{12E_sI}} = \frac{12E_sI}{c_2c_3(c_1c_2 + c_1^2)} \tag{7}$$

Substituting for I we obtain

$$G_{12}^* = \left(\frac{h^4}{c_1c_2c_3(c_1 + c_2)}\right)E_s \tag{8}$$

The shear modulus in the other two planes can be obtained by cyclic permutation as

$$G_{23}^* = \left(\frac{h^4}{c_1c_2c_3(c_2 + c_3)}\right)E_s$$

$$G_{31}^* = \left(\frac{h^4}{c_1c_2c_3(c_1 + c_3)}\right)E_s \tag{9}$$

3.2. Graded foam

The properties of a graded foam can be represented by a function of the coordinate variables x, y and z. The actual functional form depends on the application and also the type of information sought from the homogenized model of the foam. In this study, we will assume that the functions will be such that the properties calculated at the center of a cell will correspond to the properties of the homogeneous foam with that cell as its unit cell. Thus the function is actually defined only at the centers of the cells of the graded foam. Then, we will fit an equation through these points to obtain the continuous variation of properties required in the continuum model. This approach will be verified by solving some problems wherein the graded foam is subjected to some simple loading conditions and comparing the results from the macro- and micro-models.

In this study, the strut properties are taken as that of carbon foam studied earlier (Choi and Sankar, 2003), and they are listed in Table 1.

Table 1
Properties of strut material

Density, ρ_s	1750 kg/m^3
Elastic modulus, E_s	207 GPa
Poisson's ratio, v_s	0.17
Ultimate tensile strength, σ_u	3600 MPa

The relative density of functionally graded foams (FGF) depends on both the dimensions of the unit-cell and the strut thickness. Therefore, three different cases can be considered. The first case is the one where the dimensions of the unit-cell remain constant while the strut thickness varies along the x-axis. In the second case the strut thickness is kept constant with varying cell length. The last case is varying both of them. In this paper, the first two cases are studied independently. Furthermore, the material properties of functionally graded foam can be either increasing or decreasing along the x-axis. Therefore, the fracture properties of both increasing and decreasing cases are studied and compared to the homogenous case.

For the case where the strut dimensions vary, the thickness of the square strut is assumed to vary as

$$h(x) = h_0 + \alpha x \tag{10}$$

where α is a parameter that determines the degree of gradation of the properties. Then the properties such as density and elastic constants of the graded foam can be assumed to vary as given by the equations for homogeneous foams, but changing the constant h by the function $h(x)$. For example, the density variation of the foam follows from Eq. (1) and can be written as

$$\frac{\rho^*}{\rho_s} = 3\left(\frac{h(x)}{c}\right)^2 - 2\left(\frac{h(x)}{c}\right)^3 \tag{11}$$

where the unit-cell is assumed as a cube of dimension c. Similar equations can be derived for Young's modulus and shear modulus as

$$E^* = \left(\frac{h(x)}{c}\right)^2 E_s$$
$$G^* = \frac{1}{2}\left(\frac{h(x)}{c}\right)^4 E_s \tag{12}$$

Similarly we can consider the case where h, c_2 and c_3 are constants, but c_1 varies as

$$c_1^{i+1} = c_1^i + \beta \tag{13}$$

where i denotes the cell number and β is the increment in the cell length in the x direction. Again the properties of the foam will be calculated at the center of each cell using the equations for homogeneous foams as given in Eqs. (2)–(9) (see Fig. 3).

In order to verify the validity of the functional form of elastic constants that are used in the present study, a simple mechanics problem was solved using both macro- and micro-models. A rectangular solid made of the inhomogeneous foam was considered as shown in Fig. 1 (a). A uniform extension (70 µm) was applied along the upper edge of macro-model, which consists of two dimensional plane stress elements (eight nodes bi-quadratic, reduced integration element). The elastic constants of the inhomogeneous material varied as given by Eq. (12). In the FE model the elastic constants within each element were considered constant. The boundary conditions are depicted in Fig. 4. The right lower corner was fixed to prevent the rigid body motion. The resulting displacements along the boundary of the micro-model, embedded in the macro-model, were applied on the boundary of the micro-model by using the three-point interpolation. For the micromechanical model, each strut was modeled as an Euler–Bernoulli beam with two nodes and three integration point element. In order to verify the validity of properties used in the macro-model we compare the stresses in both models. In the case of macro-model the stresses are obtained as the FE output. The outputs in micro-model are the axial and transverse forces in the beam element. We convert these forces into equivalent stresses by dividing the strut cross-sectional area $c_1 \times c_3$.
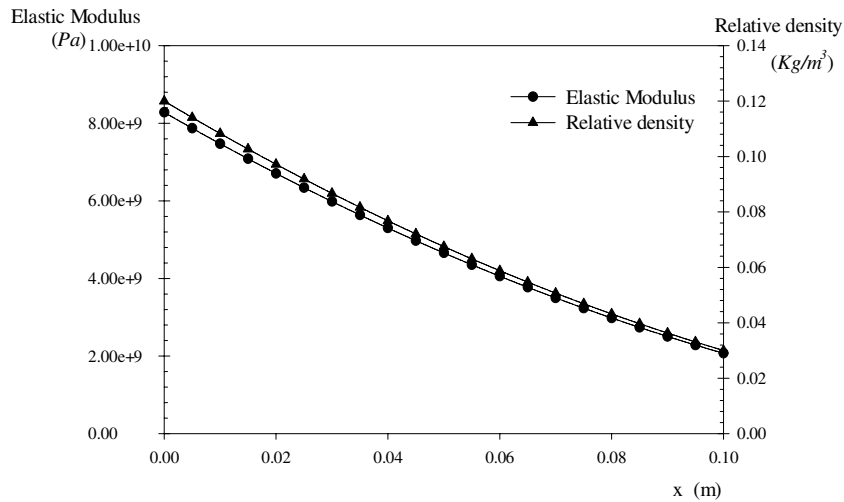
Fig. 3. Example of variation of elastic modulus and relative density for constant cell length c and $\alpha = -200 \times 10^{-6}$.
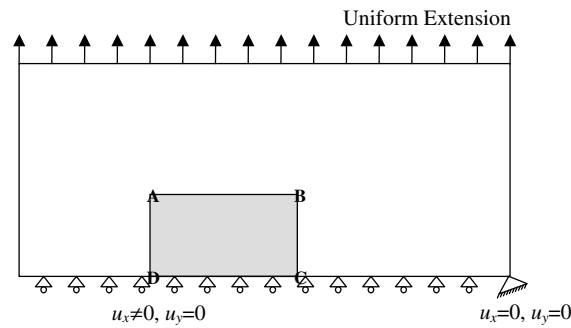

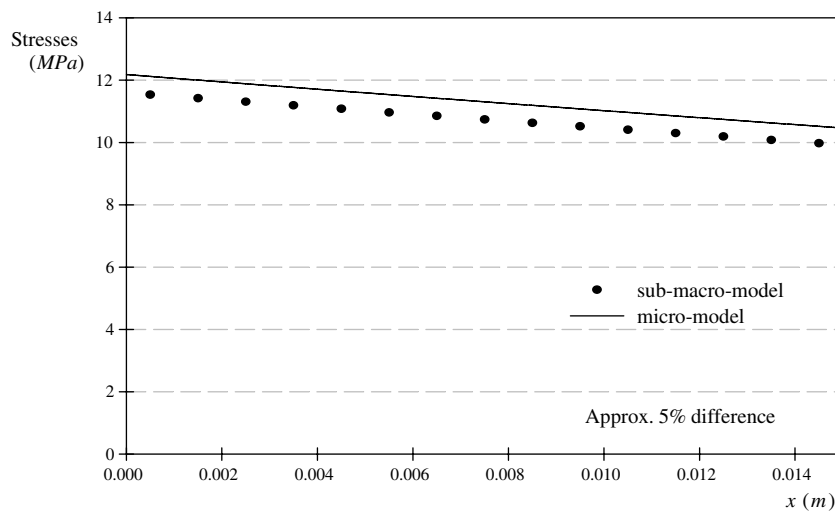Fig. 4. Boundary conditions for edge-cracked plate under uniform extension.

Fig. 5. Comparison of stresses (σ_{22}) obtained using the macro- and micro-models in graded foam with constant cell size but varying strut cross-section.
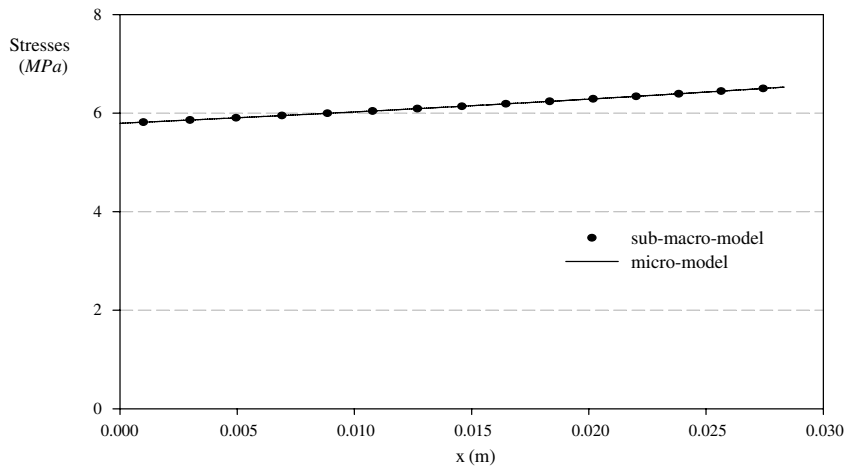
Fig. 6. Comparison of stresses (σ_{22}) obtained using the macro- and micro-models in graded foam with constant strut size but varying cell dimensions.

Fig. 4 depicts the macro-, sub-macro- and micro-models. We consider both constant cell length and constant strut size cases. In the constant cell length case the cell length is assumed as 200μm. The macro-model consists of 100×50 plane solid elements. The strut cross-section is assumed to vary as a function of x according to the equation $h(x) = h_0 + \alpha x$, where $h_0 = 40$μm and $\alpha = -200 \times 10^{-6}$. The region corresponding to the micro-model in the macro-model consists of 15×5 elements. The micro-model uses 75×25 beam elements. The results for the stress component σ_{22} from the macro- and micro-models are compared in Fig. 5. In the second case, the strut is assumed to have a square cross-section ($h = 20$ μm) and the cell length c_1 was varied along the x direction with $c_1^0 = 200$ μm and $\beta = -0.15$ μm. The dimensions of the cell in the 2 and 3 directions, c_2 and c_3, are kept constant (100 μm). The stress component σ_{22} along the upper boundary of the micro-model are compared in Fig. 6. The maximum difference in stresses between the macro- and micro-models is about 5%.

4. Fracture analysis

4.1. Macro-mechanical model

In this section, the finite element analysis (FEA) of the functionally graded foam containing a crack is performed. The purpose of the analysis is to determine the displacements along the boundaries corresponding to the micro-model for a given stress intensity factor. The macro-model for the foam is modeled using plane solid elements. An arbitrary boundary condition is applied to the macro-model and the corresponding stress intensity factor and displacements are found from the FE results. Due to symmetry about the crack plane only top half of the foam is modeled. A constant displacement in the vertical direction is applied along the top horizontal boundary as shown in Fig. 4. The J-Integral is calculated along several contours surrounding the crack tip. The displacements at the nodes on the boundary corresponding to the micro-model are obtained from the macro-model FEA results. The upper edge is loaded by a uniform displacement loading in the y-direction, and the lower edge has a zero displacement boundary condition in the y-direction to account for symmetry. The material is functionally graded by either changing the thickness of struts or changing the dimensions of the unit-cell described as before. Relative density, elastic modulus and shear modulus vary along the x-axis corresponding to the equations derived in the previous section. When, functionally graded foam is modeled as a homogeneous solid (macro-model), a material property discretization is introduced. Material properties are discretized by assigning each region along the x-axis the value of those at the centroid of the region. For exam-

ple, Fig. 7 shows the discrete elastic modulus for the 10-region model. However, the Poisson's ratio is kept constant because the effect of a variation of Poisson's ratio is negligible (Delale and Erdorgan, 1983).

A two dimensional continuum element with 8 nodes and reduced integration points is used for the plane stress problem. Generally, J-integral is not path independent for inhomogeneous material. Therefore, J-integral is expected to vary with contour numbers as shown in Fig. 8. The contour numbers represent incrementally larger contours around the crack tip. The mesh refinement governs the size and increments of contours. However, the value of J-integral for a contour very close to the crack-tip is related to the local stress intensity factor as in the case of a homogeneous material (Anals et al., 2000). Thus, energy release rate, G is identical to the value of J-integral as the path of contour approaches to zero (Gu et al., 1999). Energy release rate, G can be found by using 4th order polynomial regression of the variation of J-integrals as shown in Fig. 8. For the convergence test, the model is discretized into uniform meshes of 10×5 elements (10 regions), 20×10 (20 regions), 50×25 elements (50 regions), 100×50 (100 regions), 200×100 (200 regions) and 400×200 (400 regions). As the number of elements and regions increases, the energy release rate at the crack tip converges as shown in Fig. 9. For 100×50 elements model, the variation of J-integral is less than 0.01% compared to the 400×200 element model. Therefore, 100×50 elements model is used for further analysis in order to maintain adequate accuracy with reasonable computational time.

The stress intensity factor K_I of a functionally graded foam (two dimensional orthotropic) can be found from G using the relation (Sih and Liebowbitz, 1968).

$$G = K_I^2 \left(\frac{a_{11}a_{22}}{2}\right)^{\frac{1}{2}} \left[\left(\frac{a_{22}}{a_{11}}\right)^{\frac{1}{2}} + \frac{2a_{12} + a_{66}}{2a_{11}} \right]^{\frac{1}{2}} \tag{14}$$

where, $a_{11} = \dfrac{1}{E_1}, \quad a_{22} = \dfrac{1}{E_2}, \quad a_{33} = \dfrac{1}{E_3}$

$a_{12} = a_{23} = a_{31} = 0$

$a_{44} = \dfrac{1}{G_{23}}, \quad a_{55} = \dfrac{1}{G_{13}}, \quad a_{66} = \dfrac{1}{G_{12}}$

The stress intensity factor at the crack tip can also be obtained directly from the crack-tip stresses as

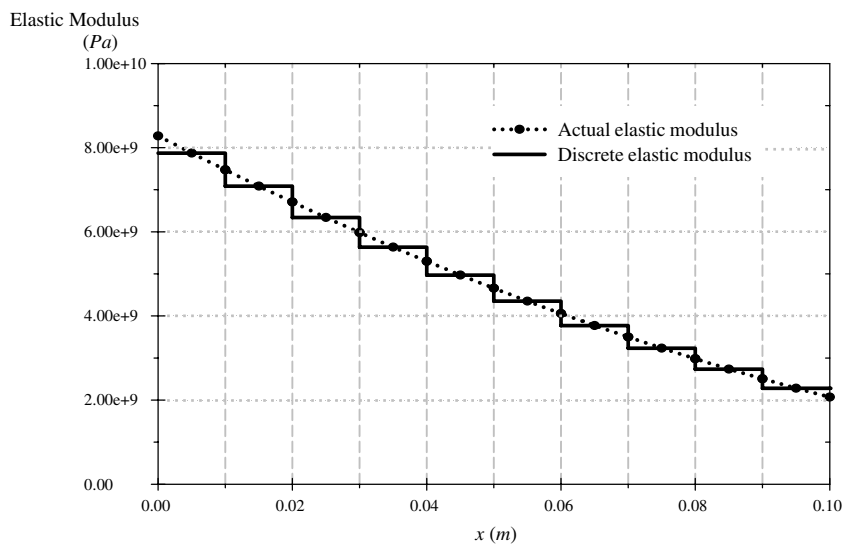$$K_I = \lim_{r \to 0} \sigma_{yy}(r, 0)\sqrt{2\pi r} \tag{15}$$

Fig. 7. Discrete elastic modulus for macro-model with 10 regions.

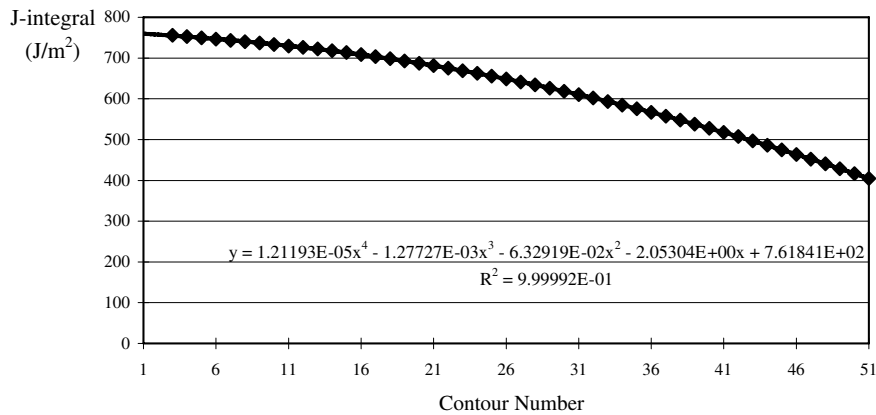Fig. 8. *J*-Integral for various contours in a macro-model containing 100×50 elements. Contour numbers increase away from the crack tip.
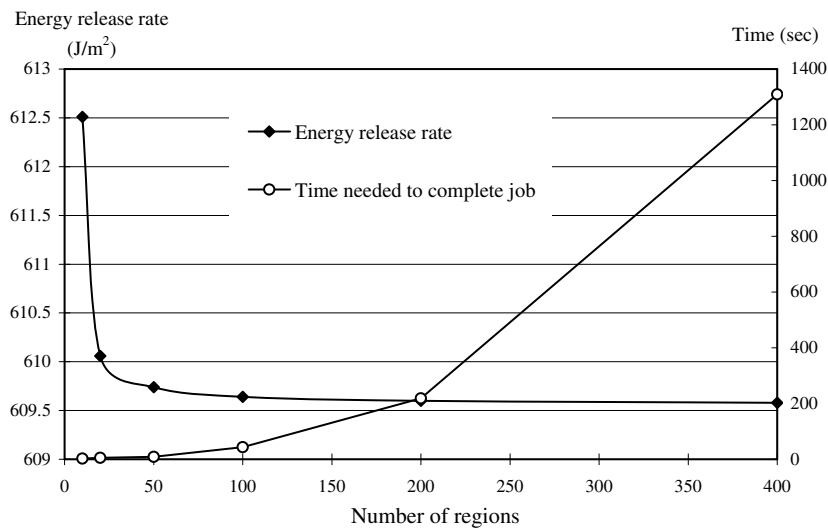

Fig. 9. Variation of energy release rate at the crack tip with various size macro-models.

Fig. 10 shows the one of the example plot of $\sigma_{yy}\sqrt{2\pi r}$ versus distance from the crack tip. A 4th order polynomial regression is also shown in Fig. 10. The *y*-intercept of the curve yields the value of K_{I}.

The stress intensity factor from both methods, *J*-Integral and stress-matching, were compared for various cases in Table 2. The maximum difference between the two methods is less than 6% for range of crack lengths studied here.

4.2. Micro-mechanical model

A portion of macro-mechanical model is taken and used for micro-model as shown in Fig. 4. As the 100×50 elements (100 regions) for macro-model and constant cell length (100 μm) for micro-model are used, one macro-model element can be replaced by 100 elements micro-model (10 beam elements in *x* and *y* directions). The displacements along the boundaries of micro-model are determined by using three points interpolation. The corresponding three points can be obtained in previous macro-model analysis. In micro-model, two-node beam elements are used to represent the foam ligaments/struts. The stresses at the crack tip can be calculated from the results for force and moment resultants obtained from the micro-model as
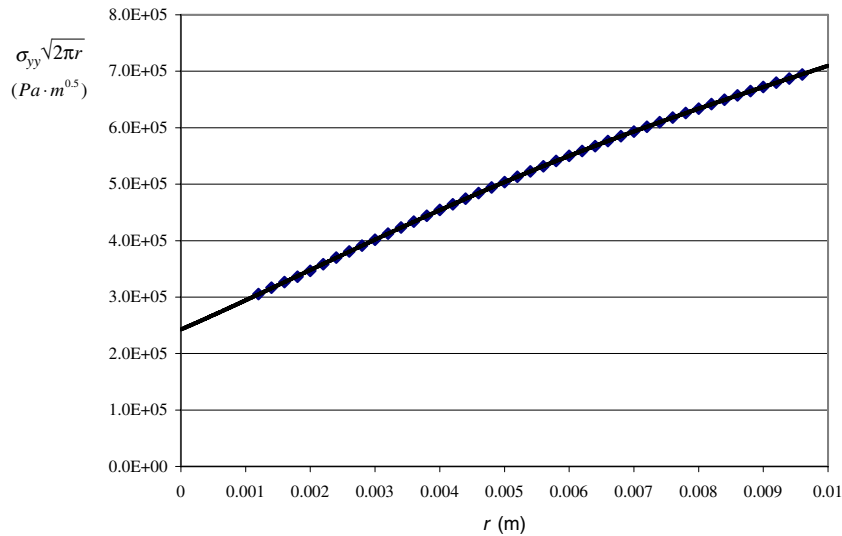
Fig. 10. Stress intensity factor from the stresses normal to the crack plane.

Table 2
Comparison between two methods

Crack length (m)	0.01	0.02	0.03	0.04	0.05
Relative density at the crack-tip	0.094582	0.085536	0.076874	0.068608	0.06075
K_I From J-Integral (Pa-m$^{1/2}$)	1.22381E+06	1.06997E+06	9.28935E+05	8.48869E+05	7.26919E+05
K_I From crack-tip stresses (Pa-m$^{1/2}$)	1.22620E+06	1.07152E+06	9.33605E+05	8.06059E+05	6.83636E+05
% difference	0.195	0.145	0.503	5.043	5.954

$$\sigma_{\text{tip}} = \frac{M_{\text{tip}} \frac{h_{\text{tip}}}{2}}{I_{\text{tip}}} \pm \frac{F_{\text{tip}}}{A_{\text{tip}}} \tag{16}$$

The fracture toughness of the foam is defined as the stress intensity factor that will cause the crack-tip struts to fail. We assume that the strut material is brittle and will fracture when the maximum principal stress exceeds the tensile strength σ_u. Since we are dealing with linear elasticity the fracture toughness can be estimated from the following relation,

$$\frac{K_I}{K_{Ic}} = \frac{\sigma_{\text{tip}}}{\sigma_u} \tag{17}$$

The convergence analysis is conducted to evaluate the variation of fracture toughness with various sizes of micro-model, 1×3 macro-model (300 elements in micro-model), 2×6 (1200), 5×15 (7500), 7×21 (14,700) and 10×30 (30,000). As model size increases, fracture toughness converges as shown in Fig. 11. For 7500 beam element model, the error in fracture toughness is less than 0.3 % compared to 30,000-beam elements model. Therefore, the 7500-model is chosen for further analysis to compromise between the accuracy and computational time. The Mode I fracture toughness with various relative densities is conducted in two different sets for the constant unit-cell case. The first set is controlling the crack length while the variation of material properties remains same. The other set is shown in Fig. 12. The crack length remains constant while the material properties are controlled to locate desired relative density at the crack tip. However, the dimensions of models are fixed ($0.1m$ by $0.5m$ for macro-model and $0.015m$ by $0.005m$ for micro-model). For the case where the unit-cell dimensions change, the number of elements both in macro-model (100×50 elements) and micro-model (150×50 elements) are fixed and the material properties at the crack tip is controlled by c_1^0 and β. Therefore, the dimensions of models are not fixed.
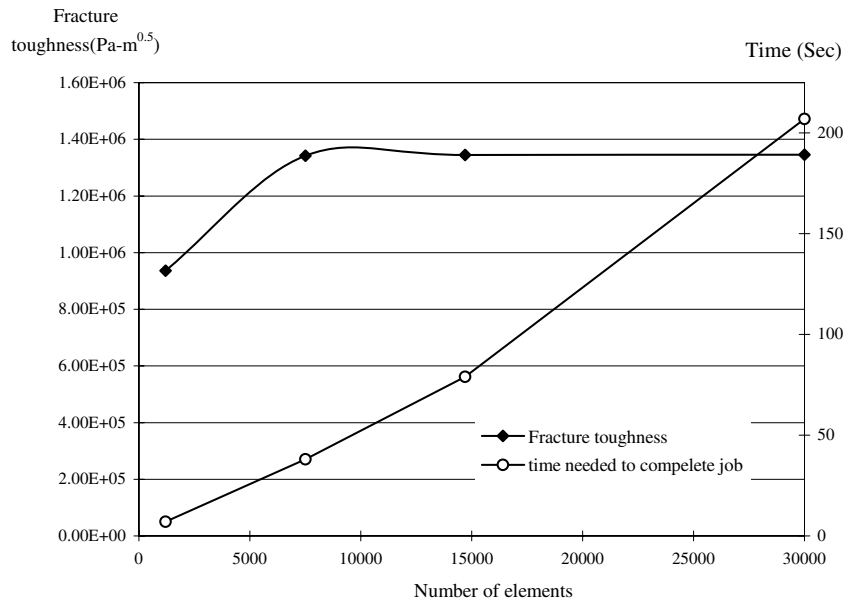
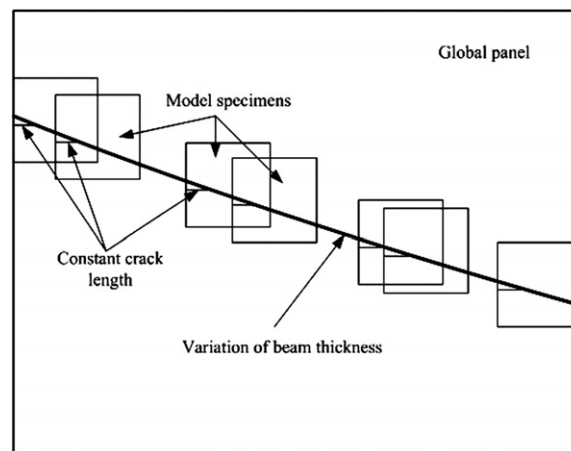Fig. 11. Variation of fracture toughness with the size of micro-models.

Fig. 12. Location of model specimens in the global panel. Each specimen is of the same size and contains a crack of given length, but the density at the crack tip varies from specimen to specimen.

5. Results and discussion

The fracture toughness of graded foams are compared to that of homogeneous foams with density same as the crack-tip density of graded foams. Both cases, increasing and decreasing densities, are considered. The results for $c = 200$ μm and for different strut thicknesses are given in Tables 3 and 4, and for $c = 100$ μm in Fig. 13. As seen from these tables and figure, the results from the present analysis are very close to those of homogeneous foam. However we see an interesting trend in Fig. 13. In both deceasing and increasing density cases, the fracture toughness deviates from that of uniform density foam for higher densities. When the density decreases along the crack path, the fracture toughness is slightly higher and vice versa.

The graded foams have constant unit-cell length ($c = 200$ μm) and the density is varied by changing the ligament cross-sectional dimensions. Results for the case of varying unit-cell dimensions are presented in Table 5

Table 3
Fracture toughness of graded and uniform foams

h_0 (μm)	Relative density at the crack-tip	Fracture toughness (Pa-m$^{1/2}$)		
		Decreasing density	Increasing density	Uniform density
26	0.028	4.52171E+05	4.56445E+05	4.51326E+05
30	0.039744	6.56122E+05	6.57406E+05	6.56114E+05
50	0.123904	2.24739E+06	2.25108E+06	2.24928E+06
60	0.179334	3.39537E+06	3.39999E+06	3.39819E+06
70	0.241664	4.77575E+06	4.78247E+06	4.77936E+06

The unit-cell dimensions and crack length are kept constant, but the strut thickness is varied. ($c = 200$μm, crack length $= 0.03m$ and $\alpha = \pm 200 \times 10^{-6}$).

Table 4
Fracture toughness of graded and uniform foams

Crack length (m)	Relative density at the crack-tip	Decreasing density	Increasing density	Uniform density
0.01	0.06075	1.10144E+06	1.03627E+06	1.03485E+06
0.02	0.068608	1.25052E+06	1.18201E+06	1.18004E+06
0.03	0.076874	1.33362E+06	1.33619E+06	1.33465E+06
0.04	0.085536	1.49961E+06	1.49980E+06	1.49878E+06
0.05	0.094582	1.67268E+06	1.67266E+06	1.67220E+06

The unit-cell dimension is kept constant but the crack length is varied. ($c = 200$ μm, $h_0 = 40$ μm and $\alpha = \pm 200 \times 10^{-6}$)
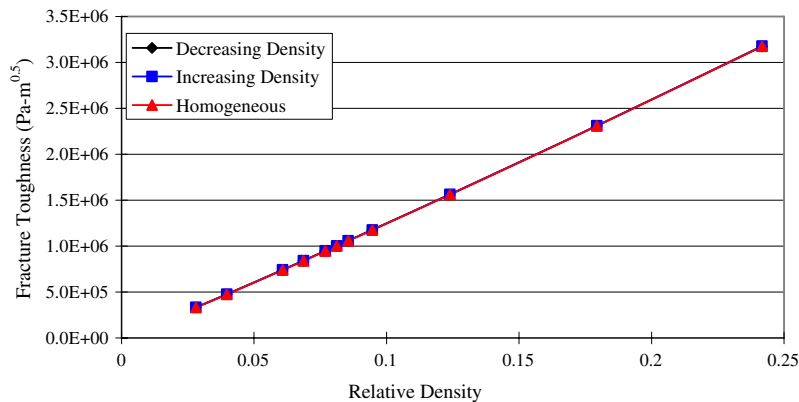

Fig. 13. Comparison of fracture toughness of graded and homogeneous foams having same density at the crack-tip. The unit-cell dimension c is kept constant at 100 μm. The strut thickness h is varied from 9.66 μm to 28.4 μm.

and also shown in Fig. 14. The results are also verifying the quite accurate results for the case where the dimensions of the unit-cell changed with constant cross-sectional area of the struts.

6. Concluding remarks

In this study, fracture toughness of functionally graded foams is predicted by employing both macro- and micro- finite element models. The macro-model in which the foam is modeled as a continuum is used to estimate the stress intensity factor at the crack tip. Both stress matching method and J-Integral are employed to compute the stress intensity factor for a given loading of the foam. The micro-model uses beam elements to model the struts and to determine the maximum stresses corresponding to the macro-stress intensity factor. From the failure criterion for the strut material the fracture toughness of the foam is estimated. It is found that the fracture toughness of functionally graded foam is approximately the same as that of homogeneous foam of same microstructure with the same density at the crack tip.

There are not many experimental works available for fracture toughness of graded foams. Recently El-Hadek and Tippur (2003) have developed a novel method to fabricate graded foams by dispersing microbal-

Table 5
Comparison of the fracture toughness for varying unit-cell dimensions with constant strut thickness ($h = 20\ \mu m$)

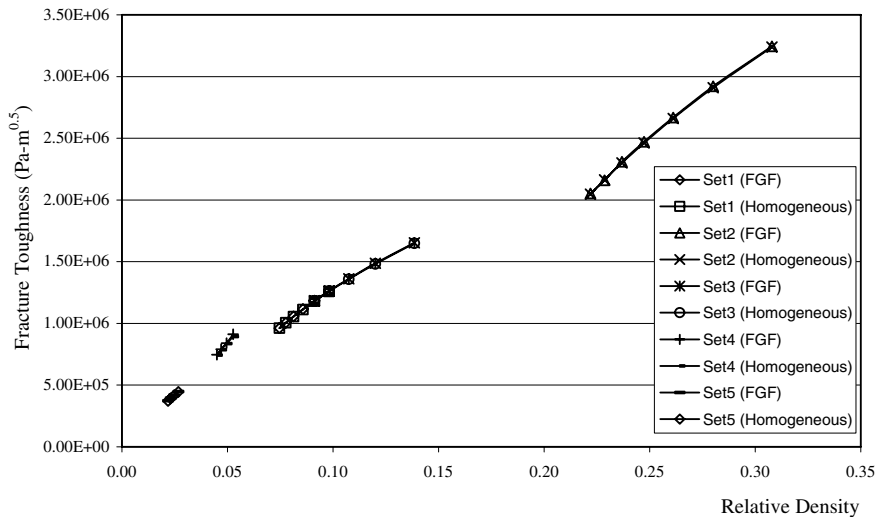| Set	β	c_1^0 (m)	c_2 (m)	c_3 (m)	Crack length in terms of number of elements	Relative density at the crack-tip	Fracture toughness (Pa-m$^{1/2}$)		% difference
							Graded foam	Homogeneous	
1	−0.15e−6	200e−6	100e−6	100e−6	10	0.0745806	9.62060E+05	9.61172E+05	0.092
					20	0.0776305	1.00630E+06	1.00531E+06	0.098
					30	0.0812704	1.05636E+06	1.05533E+06	0.097
					40	0.0856898	1.11501E+06	1.11279E+06	0.199
					50	0.0911693	1.18440E+06	1.18018E+06	0.356
					60	0.0981422	1.26090E+06	1.25952E+06	0.109
2	0.15e−6	50e−6	50e−6	50e−6	70	0.221965	2.05336E+06	2.04649E+06	0.335
					60	0.228608	2.15865E+06	2.16343E+06	0.221
					50	0.236846	2.30923E+06	2.29987E+06	0.405
					40	0.247332	2.47076E+06	2.46204E+06	0.353
					30	0.261132	2.66760E+06	2.65985E+06	0.291
					20	0.280113	2.92063E+06	2.90924E+06	0.390
					10	0.307863	3.24507E+06	3.23901E+06	0.187
3	0.15e−6	50e−6	100e−6	100e−6	50	0.0912307	1.18404E+06	1.18051E+06	0.298
					40	0.0982215	1.26352E+06	1.26041E+06	0.246
					30	0.107422	1.36134E+06	1.35823E+06	0.228
					20	0.120075	1.48715E+06	1.48204E+06	0.344
					10	0.138575	1.65340E+06	1.64829E+06	0.310
4	0.15e−6	200e−6	150e−6	100e−6	70	0.0450318	7.45601E+05	7.43076E+05	0.339
					50	0.0470359	7.89333E+05	7.85621E+05	0.470
					30	0.0495308	8.39136E+05	8.35061E+05	0.486
					10	0.0527223	9.11742E+05	8.93837E+05	1.964
5	0.15e−6	200e−6	200e−6	200e−6	70	0.0218062	3.73104E+05	3.72085E+05	0.273
					50	0.0230945	3.94813E+05	3.92956E+05	0.470
					30	0.0246984	4.19129E+05	4.17251E+05	0.448
					10	0.0267500	4.48072E+05	4.46171E+05	0.424

Fig. 14. Comparison of fracture toughness of graded and homogeneous foams. The graded foams have varying unit-cell dimensions, but constant strut cross-section $h = 20 \, \mu m$.
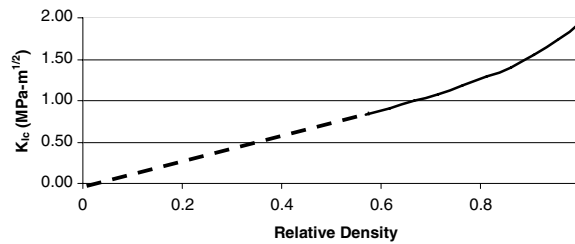

Fig. 15. Variation of fracture toughness of syntactic foams with relative density. The solid line represents the experimental results for relatively higher densities (El-Hadek and Tippur, 2003). The dotted line indicates the projected trend for low-density graded foams.

loons of varying sizes in an epoxy matrix. They measured the fracture toughness of the foam using the coherent reflection gradient sensing technique and high-speed photography. Their results are shown in Fig. 15 by the solid line.

Because the method of fabrication their material relative density ranges from 0.5 to 1.0. On the other hand in cellular materials the density usually varies from 0.02 to 0.4 depending on the microstructure. Nevertheless the trend seen in the present simulations (Fig. 13) agree qualitatively with available experimental results (Fig. 15). Hence the present work can be considered as the first step in simulating fracture in graded cellular materials in order to estimate their fracture properties.

Acknowledgements

References

Anals, G., Santare, H.M., Lambros, J., 2000. Numerical calculation of stress intensity factors in functionally graded materials. International Journal of Fracture 104, 131–143.

Choi, S., Sankar, B.V., 2003. Fracture toughness of carbon foam. Journal of Composite Materials 37 (23), 2101–2116.

Choi, S., Sankar, B.V., 2005. A micromechanical method to predict the fracture toughness of cellular materials. International Journal of Solids & Structures 42 (5–6), 1797–1817.

Delale, F., Erdorgan, F., 1983. The crack problem for nonhomogenous plane. Journal of Applied Mechanics 50, 609–614.

El-Hadek, M.A., Tippur, H.V., 2003. Dynamic fracture parameters and constraint effects in functionally graded syntactic epoxy foams. International Journal of Solids & Structures 40, 1885–1906.

Gibson, L.J., Ashby, M.F., 1998. Cellular solids: Structure and properties, 2nd ed. Cambridge University Press, Cambridge, UK, pp. 219–222.

Gu, P., Dao, M., Asaro, R.J., 1999. Simplified method for calculating the crack tip field of functionally graded materials using the domain integral. Journal of Applied Mechanics 66, 101–108.

Madhusudhana, K.S., Kitey, R., Tippur, H.V., 2004. Dynamic fracture behaviour of model sandwich structures with functionally graded core. In: Proceedings of the 22nd Southeastern Conference in Theoretical and Applied Mechanics (SECTAM), Alabama.

Sih, G.C., Liebowbitz, H., 1968Mathematical Theories of Brittle Fracture, vol. 2. Academic Press, New York, pp. 67–190.